Electron spin resonance in three spin-$\frac{1}{2}$ dimer systems: $VO(HPO_4)\cdot 0.5H_2O$, $KZn(H_2O)(VO)_2(PO_4)_2(H_2PO_4)$, and CsV_2O_5

I. S. Camara,[1] R. Gautier,[2,3] E. Le Fur,[2,3] J.-C. Trombe,[4] J. Galy,[4] A. M. Ghorayeb,[1] and A. Stepanov[1]

[1]*IM2NP, CNRS UMR 6242, Faculté des Sciences de Saint-Jérôme, Aix-Marseille Université, Case 142, F-13397 Marseille Cedex 20, France*

[2]*Ecole Nationale Supérieure de Chimie de Rennes, CNRS UMR 6226, Avenue du Général Leclerc, CS 50837, F-35708 Rennes Cedex 7, France*

[3]*Université Européenne de Bretagne, Avenue Janvier, F-35000 Rennes, France*

[4]*Centre d'Elaboration de Matériaux et d'Etudes Structurales, CNRS UPR 8011, BP 4347, 29 rue Jeanne Marvig, F-31055 Toulouse Cedex, France*

(Received 30 October 2009; published 26 May 2010)

Using X-band electron spin resonance (ESR) spectroscopy, we investigate the magnetic properties of the low-dimensional quantum-spin systems, $VO(HPO_4)\cdot 0.5H_2O$, $KZn(H_2O)(VO)_2(PO_4)_2(H_2PO_4)$, and CsV_2O_5, where the magnetic $V^{4+}(S=\frac{1}{2})$ ions are arranged in pairs. By studying the temperature dependence as well as the angular dependence of the ESR spectra, we find that these systems, which may be well described as spin-$\frac{1}{2}$ dimer systems, show a change in behavior as a function of temperature. At room temperature, in accordance with the Kubo-Tomita prediction, an exchange narrowing phenomenon takes place, whereas linewidth broadening and then the appearance of a fine structure are instead observed at helium temperatures where spins are strongly correlated.

DOI: 10.1103/PhysRevB.81.184433 PACS number(s): 76.30.−v, 75.30.Et

I. INTRODUCTION

Low-dimensional spin-gapped quantum systems have been intensively studied recently, due to the interesting low-lying magnetic excitations they exhibit. Such systems include spin-1 Haldane chains,[1,2] spin-$\frac{1}{2}$ alternating chains,[3] spin-$\frac{1}{2}$ even-leg ladders,[4] spin-Peierls systems,[5,6] or finite-size systems constituted of an even number of antiferromagnetically coupled spins.[7,8] The simplest case of this latter category is the spin-$\frac{1}{2}$ dimer structure, and many spin-gapped systems may be considered as assemblies of more or less weakly interacting dimers.[9–11] Interestingly, in the inelastic-neutron-scattering experiments, performed on these systems at low temperature, the magnetic excitation spectra (magnetic excitons) exhibit a pronounced energy dispersion indicating the existence of a *strongly correlated* ground spin state.[11,12] Since the number of magnetic excitons decreases exponentially at low temperature preventing them from collisions, their mean lifetime becomes quite large and consequently their linewidth is expected to be quite narrow making them observable in the electron spin resonance (ESR) experiment. In this work, using X-band ESR spectroscopy in the large temperature range (4–300 K), we show the existence of two quite different dynamical regimes for spin-gap systems: a stochastic one which governs the exchange narrowing of the EPR signal at high temperature and a strongly correlated one leading to magnetic excitons at low temperature.

Among the dimer structures, we shall focus in this work on three particular compounds, two of which belong to the vanadophosphate family, the vanadyl hydrogen phosphate hemihydrate $VO(HPO_4)\cdot 0.5H_2O$ (Ref. 13) and the potassium oxovanadium phosphate $KZn(H_2O)(VO)_2(PO_4)_2(H_2PO_4)$,[14] whereas the third one, CsV_2O_5,[15,16] belongs to the alkali-metal vanadate family.

The room-temperature structure of these compounds has been reported in the references mentioned above.[13–16] $VO(HPO_4)\cdot 0.5H_2O$ crystallizes in the orthorhombic structure (space group *Pmmn*) with the lattice parameters $a=7.428$ Å, $b=9.604$ Å, and $c=5.693$ Å. Figure 1 shows a schematic representation of $VO(HPO_4)\cdot 0.5H_2O$ in the (a,b) plane. V^{4+} ions (effective spin $S=\frac{1}{2}$) are arranged in pairs inside face-sharing VO_6 octahedra. The resulting basic V_2O_9 dimer unit, which is repeated along the a direction, is sketched at the top of Fig. 1. These repeated units are also corner linked via hydrogen phosphate tetrahedra in the (a,b) plane. Along the c direction, such vanadyl hydrogen phosphate layers are stacked upon each other and are linked via interlayer hydrogen bonding interactions.

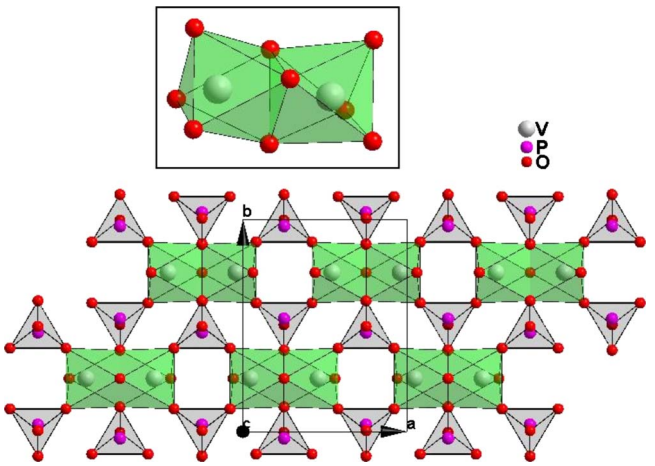

FIG. 1. (Color online) Schematic representation of $VO(HPO_4)\cdot 0.5H_2O$ in the (a,b) plane. The basic V_2O_9 dimer unit, consisting of two VO_6 octahedra sharing one face, is sketched at the top of the figure.

 ©2010 The American Physical Society

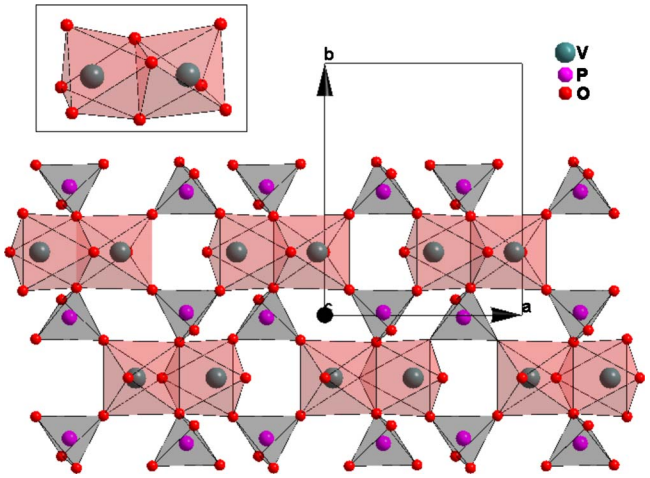

FIG. 2. (Color online) Schematic representation of the structure of $KZn(H_2O)(VO)_2(PO_4)_2(H_2PO_4)$ viewed along the c direction. The basic V_2O_9 dimer unit, consisting of two VO_6 octahedra sharing one face, is sketched at the top left corner of the figure.

The second vanadophosphate compound, $KZn(H_2O)(VO)_2(PO_4)_2(H_2PO_4)$, crystallizes in the monoclinic structure (space group $P2_1/m$) with the lattice parameters $a=7.4459$ Å, $b=9.2160$ Å, $c=9.3199$ Å, and $\beta=104.281°$. A view of the structure along the c direction is schematically represented in Fig. 2. As in the case of $VO(HPO_4)\cdot 0.5H_2O$, the magnetic V^{4+} ions are arranged in pairs within face-sharing VO_6 octahedra, forming V_2O_9 dimer units running along the a direction. Planes such as that represented in Fig. 2 are stacked upon each other and interconnected via polyhedra containing phosphorus, potassium, zinc, oxygen, and hydrogen atoms. A detailed description of the structure may be found in Ref. 14.

The third compound, the vanadate CsV_2O_5, also crystallizes in the monoclinic structure (space group $P2_1/c$) with the lattice parameters $a=7.021$ Å, $b=9.898$ Å, $c=7.783$ Å, and $\beta=90.65°$. Figure 3 shows a schematic view of the structure along the a direction. In this compound, the V^{4+} ions are also arranged in pairs (along the c direction) and sit in edge-sharing VO_5 square pyramids having their apical oxygen pointing up and down alternately. These V_2O_8 dimer units are corner connected via VO_4 tetrahedra. The layers formed by these polyhedra are held together by Cs atoms.

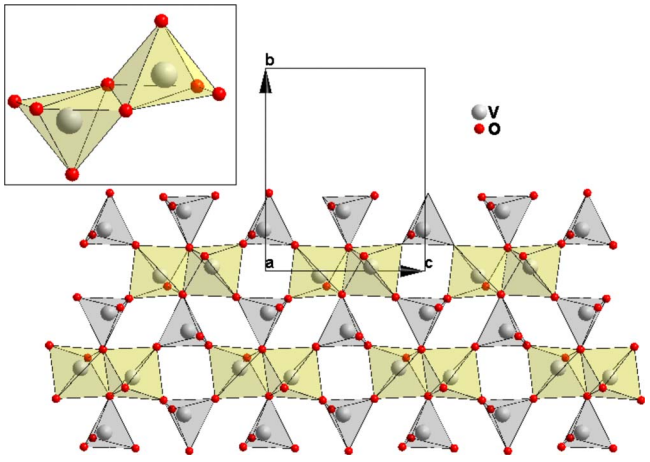

FIG. 3. (Color online) Schematic representation of CsV_2O_5 viewed along the a direction. The basic V_2O_8 dimer unit, consisting of two edge-sharing VO_5 square pyramids, is sketched at the top left corner of the figure.

The distance between V^{4+} ions within a dimer unit in the three compounds presented above is 3.10 Å, 3.057 Å, and 3.073 Å in $VO(HPO_4)\cdot 0.5H_2O$, $KZn(H_2O)\times(VO)_2(PO_4)_2(H_2PO_4)$, and CsV_2O_5, respectively. This intradimer V^{4+}-V^{4+} distance is much shorter than that between next-nearest V^{4+} neighbors lying along the direction of the chain of dimers [4.342 Å in $VO(HPO_4)\cdot 0.5H_2O$,[17] 4.389 Å in $KZn(H_2O)(VO)_2(PO_4)_2(H_2PO_4)$,[17] and 5.501 Å in CsV_2O_5 (Ref. 18)]. This is one of the reasons why these systems have been regarded, to a reasonable approximation, as assemblies of quasi-isolated spin dimers. Such a consideration is also supported by magnetic-susceptibility measurements, which can be well fitted by the expression corresponding to the susceptibility of an isolated-dimer model,[13,14,16,18–20] although, not surprisingly, other models such as the alternating chain model or the coupled alternating chain model can also satisfactorily fit the experimental results.[14,18,20] However, in most of these cases, in addition to the exchange parameter(s), the g factor of the system was also considered as a fitting parameter. Besides, most of these magnetic studies [apart from that of Ref. 20 on $VO(HPO_4)\cdot 0.5H_2O$] were performed on powder samples. This latest work[20] also presents some X-band ESR results on $VO(HPO_4)\cdot 0.5H_2O$, but this ESR study was limited to describing the behavior, as a function of temperature, of the linewidth, and g factor and absorption intensity in the 5–200 K range, without providing an interpretation for these results, apart from concluding that the temperature dependence of the ESR intensity can be well fitted by an isolated-dimer model and is consistent with the spin-gap behavior expected for a spin-$\frac{1}{2}$ dimer system. The angular dependence of the spectra was not mentioned.

In the work we present here, in order to follow the spin dynamics of spin-$\frac{1}{2}$ dimer systems through the temperature and the angular dependence of the ESR linewidth, we have performed detailed ESR measurements on single crystals of $VO(HPO_4)\cdot 0.5H_2O$, $KZn(H_2O)(VO)_2(PO_4)_2(H_2PO_4)$, and CsV_2O_5. We show in the following that, among the various results obtained, a well-marked change in behavior is noted around a particular temperature, T_{min}, in the shape of the ESR spectra and also in the temperature and angular dependence of the ESR linewidth.

II. EXPERIMENTAL DETAILS

Single crystals of $VO(HPO_4)\cdot 0.5H_2O$ and $KZn(H_2O)(VO)_2(PO_4)_2(H_2PO_4)$ were prepared at the Institute of Chemistry in Rennes, France, following the synthesis details presented in Refs. 13 and 14, respectively. The CsV_2O_5 single crystals were synthesized in the Centre for material preparation and structural studies in Toulouse, France, following the procedure described in Ref. 15. The samples used for the measurements had a platelike shape

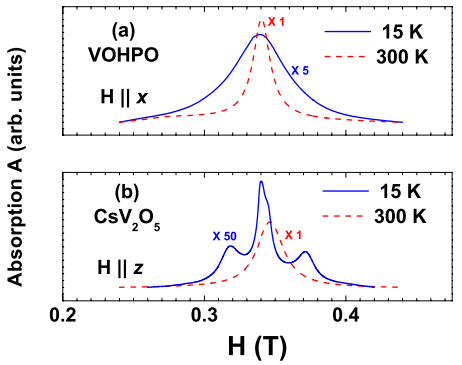

FIG. 4. (Color online) Above: ESR absorption spectra in $VO(HPO_4)\cdot 0.5H_2O$ (abbreviated as VOHPO) at 300 K (dashed curve; Lorentzian form) and 15 K (continuous curve; no longer Lorentzian). Below: ESR absorption spectra in CsV_2O_5 at 300 K (dashed curve; Lorentzian form) and 15 K (continuous curve; no longer Lorentzian).

with approximate dimensions of about $1\times 1\times 0.1$ mm^3.

The ESR measurements were performed on a BRUKER EMX spectrometer operating in the X-band (ν=9.4 GHz). The spectrometer is equipped with an Oxford Instruments continuous He-flow cryostat, enabling measurements in the temperature range $4.2\leq T\leq 300$ K. The spectrometer is also equipped with a goniometer which allows us to select a precise orientation for the sample, that can be defined to within a quarter of a degree.

III. RESULTS AND DISCUSSION

A. *g* factor and static susceptibility deduced from ESR

For all three compounds studied, the acquired ESR spectra, which are recorded in the form of the derivative of absorption with respect to the magnetic field H, can be well fitted, in the case of high temperatures, by the derivative with respect to H of a Lorentzian function.

At low temperatures, however, the shape of the spectra deviates from a Lorentzian form (see Fig. 4 for an illustration). In that case, the static susceptibility was determined from a double integration of the ESR signal.

Before acquiring spectra as a function of temperature, we have determined, at room temperature and for each of the samples studied, the three magnetic axes which we shall denote by **x**, **y**, and **z** axes. These axes were determined by following the angular variation in the g factor. The **z** axis was found to be perpendicular to the platelike plane of the samples, whereas **x** and **y** axes were found to lie within that plane. The g-factor values as measured along these magnetic axes are denoted by g_x, g_y, and g_z. The room-temperature values of these quantities are given in the upper part of Table I.

Whereas g_x and g_y differ from each other by only less than 0.4%, they differ from g_z by more than 2%. This allows us to take the hypothesis of an axial symmetry for these systems.

The behavior of the temperature dependence of the static susceptibility of each of the three compounds, as determined from a double integration of the ESR signal, is typical of a low-dimensional spin-gap system: as the temperature decreases, the susceptibility first increases gradually, then passes through a maximum, before falling down toward zero. In the case of $VO(HPO_4)\cdot 0.5H_2O$ and $KZn(H_2O)(VO)_2(PO_4)_2(H_2PO_4)$, the raw susceptibility data show a slight upturn below 10 K, which can be safely attributed to magnetic impurities such as isolated V^{4+} ions. This low-temperature part of the raw susceptibility is shown in Fig. 5, for temperatures $T\leq 20$ K. The figure also shows that the upturn below 10 K can be well reproduced by a Curie-

TABLE I. Upper part: the g-factor values measured at room temperature in the three magnetic directions **x**, **y**, and **z**. Lower part: the intradimer exchange coupling in the same directions, J_x, J_y, and J_z, as determined by fitting the susceptibility curve to a dimer model expressed by Eq. (1) (see text for details). k_B is Boltzmann's constant. (**A**), (**B**), and (**C**) denote the compounds $VO(HPO_4)\cdot 0.5H_2O$, $KZn(H_2O)(VO)_2(PO_4)_2(H_2PO_4)$, and CsV_2O_5, respectively.

	(**A**)	(**B**)	(**C**)
g_x	1.973	1.973	1.974
g_y	1.981	1.979	1.975
g_z	1.933	1.934	1.937
$-\frac{J_x}{k_B}$ (K)	97	83	148
$-\frac{J_y}{k_B}$ (K)	96	82	144
$-\frac{J_z}{k_B}$ (K)	96	81	145

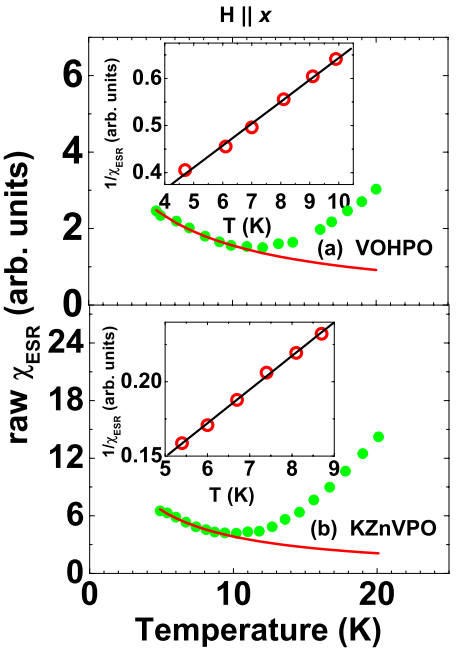

FIG. 5. (Color online) Temperature dependence, for $T\leq 20$ K, of the raw ESR susceptibility of (a) $VO(HPO_4)\cdot 0.5H_2O$ (abbreviated as VOHPO) and (b) $KZn(H_2O)(VO)_2(PO_4)_2(H_2PO_4)$ (abbreviated as KZnVPO), measured for H parallel to the **x** direction (full circles) and that of the susceptibility of impurities, χ_{imp} (continuous curves). Insets: linear fits of the inverse of the raw susceptibility showing a Curie-Weiss behavior below 10 K.

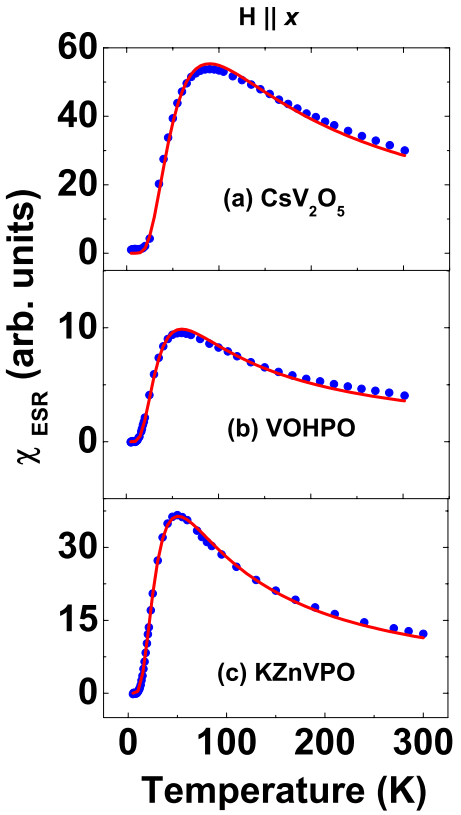

FIG. 6. (Color online) Full circles: temperature dependence, for $4.2 \leq T \leq 300$ K, of the corrected static susceptibility of (a) CsV_2O_5, (b) $VO(HPO_4)\cdot 0.5H_2O$, and (c) $KZn(H_2O)\times(VO)_2(PO_4)_2(H_2PO_4)$, as deduced from the ESR measurements for H parallel to the **x** direction, after subtraction of the susceptibility of impurities. Continuous curves: fits of the experimental data to the theoretical temperature dependence of spin-$\frac{1}{2}$ dimer systems as expressed by Eq. (1).

Weiss behavior expressed by $\chi_{imp}=C_{imp}/(T-T_{imp})$ and representing the temperature dependence of the susceptibility of the magnetic impurities. The data shown in Fig. 5 correspond to the case where H is parallel to the **x** direction. Similar behavior is also obtained in **y** and **z** directions.

Once the susceptibility of the impurities is subtracted from the raw susceptibility data, the static susceptibility corresponding to each of the pure materials studied is then obtained (in the case of CsV_2O_5, there was no need for such a correction). This corrected susceptibility is plotted in the whole temperature range ($4.2 \leq T \leq 300$ K) in Fig. 6.

The corrected susceptibility curves corresponding to H parallel to **y** and **z** directions are also similar to those presented in Fig. 6.

Considering the presence of V^{4+}-ion dimers in the three compounds studied, we have used here the simplest model in order to fit the susceptibility data, namely, the isolated-dimer model, where the exchange-interaction term in the Hamiltonian would be given by $-JS_1S_2$, the exchange coupling parameter J being restricted to nearest neighbors (intradimer) only. Obviously, a more realistic model should include couplings to more distant neighbors as well. However, as one can see here, this simple spin-$\frac{1}{2}$ isolated-dimer model is able to reproduce the experimental data fairly well. The susceptibility of a system of N isolated dimers may be expressed by

$$\chi_{dimers} = \frac{2N(g\beta)^2}{k_BT\left[3+\exp\left(-\frac{J}{k_BT}\right)\right]}, \quad (1)$$

where β is the Bohr magneton and k_B is Boltzmann's constant. The continuous curves in Fig. 6 represent fits of the experimental data using Eq. (1). For each curve, the g-factor value used in the fit is the value deduced from the ESR measurement and which has been given in the upper part of Table I. The values of the exchange coupling parameter resulting from the fit are given in the lower part of Table I for each of the three compounds and in all three magnetic directions. We may easily notice that, for each compound, the exchange coupling parameter values in all three directions are almost the same. This indicates that the intradimer exchange coupling is quasi-isotropic and is thus more significant than any other term in the Hamiltonian of the system. Indeed, this can be easily checked by a simple estimate of the anisotropic terms of the Hamiltonian. The most significant anisotropic interactions are usually (i) the single-ion anisotropy, (ii) the dipole-dipole interaction (symmetric exchange anisotropy), and (iii) the Dzyaloshinskii-Moriya (DM) interaction.[21,22] Considering (i), the single-ion anisotropy term is absent for $S=\frac{1}{2}$. Now if we consider (ii) and (iii), the dipolar interaction and the DM interaction may be estimated[22] as $(\frac{\Delta g}{g})^2 J$ and $(\frac{\Delta g}{g})J$, respectively, where Δg is the deviation of the g factor from the free-electron value. This rough estimation gives a dipolar interaction of about $10^{-3}J$ and a DM term of the order of $3\times 10^{-2}J$. Given the J values of Table I, these interactions may obviously be considered as negligible. Having said that, one should nevertheless bear in mind that a system of completely isolated dimers is not quite realistic, and some interdimer coupling, as weak as it may be, should be considered. This aspect of the precise determination of the exchange interactions will be treated in detail in a future publication. In the rest of this paper here we shall focus on the information we may get concerning the spin dynamics in the systems that we are studying, essentially out of the behavior of the ESR spectral linewidth.

B. ESR linewidth

One of the remarkable features shown by the ESR spectra of our systems is that, around a certain temperature, which we shall denote by $T_{\min}$, a notable change in the behavior of the linewidth occurs. This is shown in Fig. 7 for (a) CsV_2O_5, (b) $VO(HPO_4)\cdot 0.5H_2O$, and (c) $KZn(H_2O)(VO)_2(PO_4)_2(H_2PO_4)$, in all three directions, **x**, **y**, and **z**.

It is clear from this figure that there are two different regimes in the temperature dependence of the ESR linewidth: (i) a high-temperature regime in which a slow decrease in the linewidth is observed with decreasing temperature and (ii) a low-temperature regime where a sudden increase in the linewidth is instead observed. The tempera-

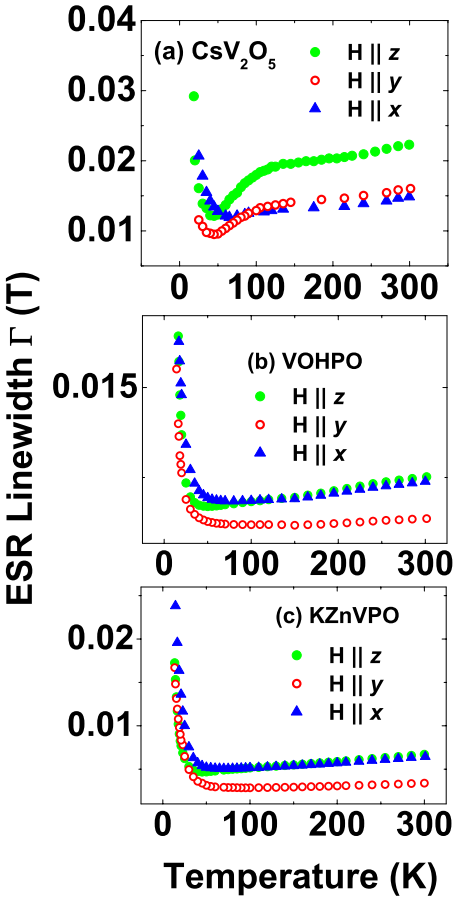

FIG. 7. (Color online) Temperature dependence of the ESR linewidth of (a) CsV_2O_5, (b) $VO(HPO_4)\cdot 0.5H_2O$, and (c) $KZn(H_2O)(VO)_2(PO_4)_2(H_2PO_4)$, in all three directions, **x**, **y**, and **z**. The lowest temperature for the plotted data is 19 K in (a) and 14 K in (b) and (c).

ture, T_{min}, at which this change occurs seems to be approximately about 50 K, although, strictly speaking, it is slightly different as we move from a compound to another. It should be noted, however, that this temperature also corresponds approximately to that below which the ESR spectra are no longer Lorentzian. The change in shape (from Lorentzian to non-Lorentzian) has already been mentioned earlier (see Fig. 4).

We attribute this change in behavior to the fact that the exchange narrowing mechanism, which prevails at high temperature as predicted by the theory of Kubo and Tomita,[23] is no longer effective at low temperature, hence showing, below approximately 50 K, important linewidth broadening as well as a departure from the Lorentzian shape of the spectra. Evidence for the nonapplicability, at low temperature, of the Kubo-Tomita model comes not only from the temperature dependence of the ESR spectra but also from their angular dependence at different temperatures as we shall soon see.

Indeed, the Kubo-Tomita approach[23] expresses the ESR linewidth at infinite temperature in the case of a sufficiently strong exchange interaction (which we shall denote by J_{ex}) as

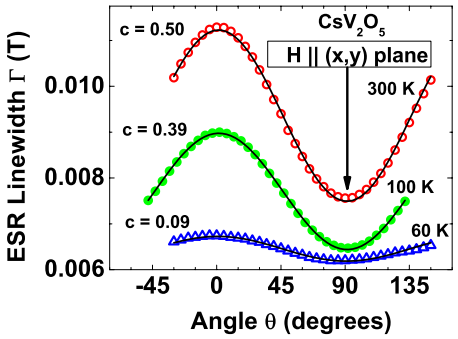

FIG. 8. (Color online) Angular dependence of the ESR linewidth of CsV_2O_5 at 300, 100, and 60 K. Symbols represent experimental data points; solid lines are fits to the data using Eq. (3).

$$\Gamma_\infty = \frac{d^2}{J_{ex}}[1+\cos^2(\theta)], \tag{2}$$

where d is a term representing the anisotropic interactions and θ is the angle between the applied magnetic field and the anisotropy direction. In order to follow the applicability of this theory as the temperature decreases, we have studied the angular dependence of the ESR linewidth at different temperatures. We have then fitted the experimental data using a modified version of Eq. (2), which we write as follows:

$$\Gamma = \Gamma_{min}[1+c\,\cos^2(\theta)], \tag{3}$$

where c is a factor which we have introduced in order to take account of the variation with temperature of the angular dependence of the linewidth.

As an example, we show in Fig. 8 the angular dependence of the ESR linewidth in CsV_2O_5 at three different temperatures, 300, 100, and 60 K. Symbols represent experimental data points, whereas the continuous lines are fits to the experimental data using Eq. (3).

It is clear from Fig. 8 that the angular dependence of the linewidth satisfactorily follows that predicted by Kubo-Tomita in the high-temperature regime with a c factor that decreases with decreasing temperature. The trend followed by the c-factor value indicates that the Kubo-Tomita angular dependence will no longer hold below a temperature approaching approximately 50 K, the same temperature which we had previously denoted as T_{min} and below which an important line broadening was observed in Fig. 7.

In fact, as the temperature decreases below T_{min}, the central resonance widens and then splits up into two main resonance signals on either side of what was, at high temperature, the unique central signal. As an example of this behavior, we show in Fig. 9 the ESR spectra of CsV_2O_5 taken at 15 K for different values of the angle θ varying between 0° and 90°.

We interpret this splitting of the main resonance as the observation of a fine structure of a magnetic exciton spectrum at $q=0$. Such a splitting may be expected if the anisotropic terms in the Hamiltonian gain importance with respect to the isotropic terms. Indeed, since in the case of an $S=\frac{1}{2}$ system the lowest excited state is a triplet state, even a small magnetic anisotropy will remove the degeneracy in the reso-

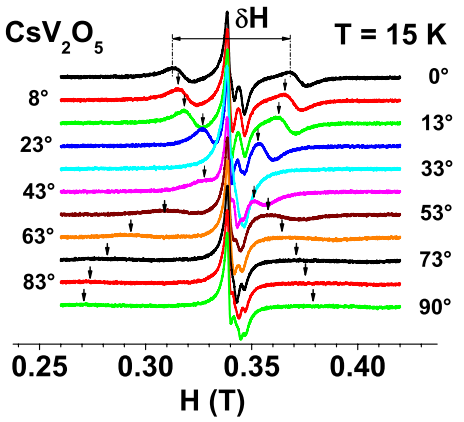

FIG. 9. (Color online) ESR spectra of CsV_2O_5 taken at 15 K for different values of θ between 0° and 90°. Small arrows indicate the positions of the split-up resonance lines.

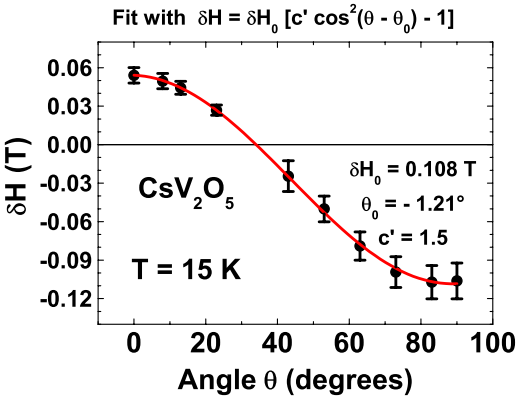

FIG. 10. (Color online) Angular dependence of the splitting δH in CsV_2O_5.

nance line position (resonance field), so that the transitions $S_z=-1$ to $S_z=0$ and $S_z=0$ to $S_z=+1$ will occur at different magnetic fields.

If we denote the field separation between the two resonance peaks by δH, then their energetic separation, taking into account the orientation of the magnetic field with respect to the anisotropy axis, is given by (see, e.g., Ref. 24)

$$g\beta\delta H = D[3\cos^2(\theta) - 1], \tag{4}$$

where D is a fine-structure constant. Equation (4) indicates that, for $\theta=0$, the energetic separation between the two peaks gives twice the value of D.

As we show in Fig. 10, we may easily check that the field separation, δH, verifies reasonably well a slightly modified version of Eq. (4), written as

$$\delta H = \delta H_0[c'\cos^2(\theta - \theta_0) - 1], \tag{5}$$

where c', θ_0, and $\delta H_0 = 3D/c'g\beta$ are parameters deduced from the fit.

It is clear from Fig. 10 that the separation between the two resonance peaks follows Eq. (5) quite well, yielding a value of δH_0 on the order of 0.1 T, which leads to a value of approximately 0.03 K for D in accordance with our estimation of the magnetic dipolar anisotropy in this compound.

The change in the angular dependence of the linewidth, from a $[1+c\cos^2(\theta)]$ dependence at high temperature to a $[c'\cos^2(\theta)-1]$ dependence at low temperature, constitutes a further important indication that the exchange narrowing mechanism predicted by Kubo-Tomita in the high-temperature regime is no longer effective at low temperature.

IV. SUMMARY AND CONCLUSION

Using X-band ESR spectroscopy on three spin-$\frac{1}{2}$ dimer systems, $VO(HPO_4)\cdot 0.5H_2O$, $KZn(H_2O)\times(VO)_2(PO_4)_2(H_2PO_4)$, and CsV_2O_5, we have shown that, for all of these three compounds, (i) a quasiaxial symmetry may be assumed, judging from the angular dependence of the g factor, (ii) the temperature dependence of the susceptibility data deduced from the ESR spectra may be satisfactorily fitted with that of an isolated-dimer model, giving a quasi-isotropic, antiferromagnetic, intradimer exchange interaction term, J, on the order of 96 K, 82 K, and 145 K, in the three studied systems, respectively, and (iii) most importantly, the temperature dependence of the linewidth as well as its angular dependence at various temperatures indicate a distinct change in magnetic behavior below a temperature, T_{min}, of approximately 50 K. We interpret this change in behavior as being related to the fact that the exchange narrowing mechanism predicted by Kubo and Tomita[23] in the high-temperature regime is no longer effective at low temperatures. Instead, a strongly correlated spin dynamics leading to magnetic excitons is the most suitable physical picture for this temperature range. We wish to mention at this stage that the existence of a splitting in the resonance line at low temperature in the ESR spectra of $VO(HPO_4)\cdot 0.5H_2O$ has been briefly mentioned in a single sentence of Ref. 20, and more clear evidence for a similar feature has also been reported in another spin-$\frac{1}{2}$ dimer system, $BaCuSi_2O_6$ (Refs. 25 and 26). However, these latter two references discuss this low-temperature splitting in terms of "motional exchange." In our work here we propose another interpretation. We wish to stress that our study leads us to the conclusion that two different regimes govern the spin dynamics in our dimer systems: a high-temperature stochastic regime that can be reasonably well described by the Kubo-Tomita exchange narrowing picture, and a low-temperature totally different regime where spins are strongly correlated. Finally, it is important to mention that the behavior which we observe (particularly the temperature dependence and the angular dependence of the ESR linewidth) is common between all three systems we have considered and seems to be the case in the $BaCuSi_2O_6$ system as well,[25,26] and hence may be regarded as a general feature that should be expected in all spin-gap systems. More experimental work (neutron scattering, etc.) and theoretical work should be done in order to confirm this point.

[1] M. Date and K. Kindo, Phys. Rev. Lett. **65**, 1659 (1990).
[2] J. Darriet and L. P. Regnault, Solid State Commun. **86**, 409 (1993).
[3] G. Xu, C. Broholm, D. H. Reich, and M. A. Adams, Phys. Rev. Lett. **84**, 4465 (2000).
[4] M. Azuma, Z. Hiroi, M. Takano, K. Ishida, and Y. Kitaoka, Phys. Rev. Lett. **73**, 3463 (1994).
[5] B. Grenier, P. Monod, M. Hagiwara, M. Matsuda, K. Katsumata, S. Clément, J.-P. Renard, A. L. Barra, G. Dhalenne, and A. Revcolevschi, Phys. Rev. B **65**, 094425 (2002).
[6] D. V. Zakharov, J. Deisenhofer, H.-A. Krug von Nidda, P. Lunkenheimer, J. Hemberger, M. Hoinkis, M. Klemm, M. Sing, R. Claessen, M. V. Eremin, S. Horn, and A. Loidl, Phys. Rev. B **73**, 094452 (2006).
[7] A. A. Belik, M. Azuma, A. Matsuo, T. Kaji, S. Okubo, H. Ohta, K. Kindo, and M. Takano, Phys. Rev. B **73**, 024429 (2006).
[8] A. M. Ghorayeb, M. Costes, M. Goiran, J.-M. Broto, S. Schäfer, R. Hayn, J. Richter, P. Millet, and A. Stepanov, Phys. Rev. B **77**, 224434 (2008).
[9] T. Nakajima, H. Mitamura, and Y. Ueda, J. Phys. Soc. Jpn. **75**, 054706 (2006).
[10] Y. Nakagawa, T. Kashiwagi, H. Yamaguchi, S. Kimura, Z. Honda, K. Yamada, K. Kindo, and M. Hagiwara, J. Phys. Soc. Jpn. **75**, 124708 (2006).
[11] Y. Sasago, K. Uchinokura, A. Zheludev, and G. Shirane, Phys. Rev. B **55**, 8357 (1997).
[12] M. Nishi, O. Fujita, and J. Akimitsu, Phys. Rev. B **50**, 6508 (1994).
[13] J. W. Johnson, D. C. Johnston, A. J. Jacobson, and J. F. Brody, J. Am. Chem. Soc. **106**, 8123 (1984).
[14] S. Messaoudi, E. Furet, R. Gautier, E. Le Fur, O. Peña, and J. Y. Pivan, Chem. Mater. **16**, 435 (2004).
[15] K. Waltersson and B. Forslund, Acta Crystallogr., Sect. B: Struct. Sci. **33**, 789 (1977).
[16] J. Mur and J. Darriet, C. R. Acad. Sci., Ser. II: Mec., Phys., Chim., Sci. Terre Univers **300**, 599 (1985).
[17] E. Le Fur (unpublished).
[18] R. Valentí and T. Saha-Dasgupta, Phys. Rev. B **65**, 144445 (2002).
[19] M. Isobe and Y. Ueda, J. Phys. Soc. Jpn. **65**, 3142 (1996).
[20] J. Cao, J. T. Haraldsen, S. Brown, J. L. Musfeldt, J. R. Thompson, S. Zvyagin, J. Krzystek, M.-H. Whangbo, S. E. Nagler, and C. C. Torardi, Phys. Rev. B **72**, 214421 (2005).
[21] D. Dzyaloshinsky, J. Phys. Chem. Solids **4**, 241 (1958).
[22] T. Moriya, Phys. Rev. Lett. **4**, 228 (1960); Phys. Rev. **120**, 91 (1960).
[23] R. Kubo and K. Tomita, J. Phys. Soc. Jpn. **9**, 888 (1954); P. W. Anderson and P. R. Weiss, Rev. Mod. Phys. **25**, 269 (1953).
[24] A. Abragam and B. Bleaney, *Electron Paramagnetic Resonance of Transition Ions* (Clarendon, Oxford, 1970).
[25] S. E. Sebastian, P. Tanedo, P. A. Goddard, S.-C. Lee, A. Wilson, S. Kim, S. Cox, R. D. McDonald, S. Hill, N. Harrison, C. D. Batista, and I. R. Fisher, Phys. Rev. B **74**, 180401(R) (2006).
[26] S. A. Zvyagin, J. Wosnitza, J. Krzystek, R. Stern, M. Jaime, Y. Sasago, and K. Uchinokura, Phys. Rev. B **73**, 094446 (2006).